

## Supporting Information

### **Biphasic Synthesis of Biodegradable Urchin-Like Mesoporous Organosilica Nanoparticles for Enhanced Cellular Internalization and Precision Cascaded Therapy**

**Yaya Cheng,<sup>a,c</sup> Xiangyu Jiao,<sup>a</sup> Zhantong Wang,<sup>c</sup> Orit Jacobson,<sup>c</sup> Maria A Aronova,<sup>d</sup> Yuanyuan Ma,<sup>c</sup> Liangcan He,<sup>c</sup> Yijing Liu,<sup>c</sup> Wei Tang,<sup>c</sup> Liming Deng,<sup>c</sup> Jianhua Zou,<sup>c</sup> Zhen Yang,<sup>c</sup> Mingru Zhang,<sup>c</sup> Yongqiang Wen,<sup>\*a</sup> Wenpei Fan,<sup>\*b</sup> and Xiaoyuan Chen<sup>\*c,e</sup>**

<sup>a</sup> *Department of Chemistry & Biological Engineering, Beijing Key Laboratory for Bioengineering and Sensing Technology, University of Science & Technology Beijing, Beijing 100083, China*  
*E-mail: wyq\_wen@iccas.ac.cn*

<sup>b</sup> *State Key Laboratory of Natural Medicines and Jiangsu Key Laboratory of Drug Discovery for Metabolic Diseases, Center of Advanced Pharmaceuticals and Biomaterials, China Pharmaceutical University, Nanjing 210009, China*  
*E-mail: wenpei.fan@cpu.edu.cn*

<sup>c</sup> *Laboratory of Molecular Imaging and Nanomedicine, National Institute of Biomedical Imaging and Bioengineering National Institutes of Health, Bethesda, MD 20892, USA*

<sup>d</sup> *Laboratory of Cellular Imaging and Macromolecular Biophysics National Institute of Biomedical Imaging and Bioengineering (NIBIB) National Institutes of Health (NIH), Bethesda, MD 20892, USA*

<sup>e</sup> *Yong Loo Lin School of Medicine and Faculty of Engineering, National University of Singapore, Singapore 119228, Singapore*  
*E-mail: chen.shawn@nus.edu.sg*

## ***Part A: Experimental Section***

**Synthesis of SONS.** Monodispersed solid organosilica nanoparticles were prepared according to the typical Stöber method. Typically, 40 mL of ethanol, 1.5 mL of water and a certain volume (1.3, 1.8, 2.3, 2.5 mL) of anhydrous ammonia were mixed and stirred gently for 5 minutes, followed by a quick addition mixed solution of TEOS and BTDS. Then the mixed system was heated to 55 °C stirred for 4 h, and the resulting SONS were collected by centrifugation and washed with ethanol several times, and dispersed in 15 mL ultrapure water.

**Synthesis of MONs.** Typically, 2 g of CTAC and a certain mass (0.1, 0.08, 0.06, 0.05 g) of TEA were first mixed in 20 mL of ultrapure water and stirred vigorously for 0.5 h at 80 °C oil base, and then the mixed silica precursors of TEOS and BTDS (1 mL) was added dropwise for another 4 h of reaction. Afterward, the resulting MONs were obtained after centrifugation and then washed with ethanol several times. The CTAC template of MONs was extracted in ethanol (100 mL) containing concentrated HCl (37%) (10 mL) and heated at 78 °C for 12 h. The extraction procedure was repeated at least two times to guarantee the complete removal of CTAC, and the CTAC-free MONs products were redispersed in 15 mL of ultrapure water.

**Observation of intracellular H<sub>2</sub>O<sub>2</sub>.** The intracellular H<sub>2</sub>O<sub>2</sub> was measured and observed by using an intracellular H<sub>2</sub>O<sub>2</sub> probe. U87MG cells were seeded in chambered coverglass and incubated at 37 °C for 24 h. Then the old media were replaced by DMEM media of UMONs, UMONs-Au, UMONs-LA and UMONs-LA-Au. After another 4 h of co-incubation, 0.001 mL of fluorescent H<sub>2</sub>O<sub>2</sub> sensor in DMSO was added and incubated for another 1 h, and the cell nucleus was stained by DAPI. Fluorescent images of intracellular H<sub>2</sub>O<sub>2</sub> were captured by confocal microscopy.

**In vitro toxicity evaluation of UMONs.** U87MG cells were seeded into 96-well cell-culture plates at a density of  $1 \times 10^4$  per well and incubated at 37 °C under 5% CO<sub>2</sub> for 24 h. Different gradient concentrations (7.5, 15.5, 31.5, 62.5, 125, 250, 500 µg/mL) of UMONs in DMEM media were separately added to the wells and allowed to co-incubate for 24 h. Afterward, the old media were removed and replenished with 5 mg/mL MTT (Thiazolyl Blue Tetrazolium Bromide) in 0.1 mL DMEM media for another 4 h of co-incubation. The old DMEM media containing MTT were then substituted by 0.1 mL DMSO, and the absorbance was monitored at 490 nm. The cytotoxicity was calculated by the viabilities of UMONs-treated cells versus those of untreated control cells.

**Preparation of  $^{64}\text{Cu}$ -labeled UMONs.** 25 mg of UMONs were ultrasonicated and dispersed in 70 mL of ethanol. 0.1 mL of MPTES and 0.15 mL of  $\text{NH}_4\text{OH}$  were added dropwise into the above solution and stirred at room temperature. After reacting for 12 h, the nanoparticles were washed with ethanol and water, and the final SH-modified UMONs products were dispersed in 2 mL MES buffer (10 mmol/L). Specifically,  $^{64}\text{Cu}$  was used to label UMONs-SH by making use of the strong chelating affinity of thiol groups to radionuclides. Thereafter, 0.5 mCi of  $^{64}\text{Cu}$  was transferred to the mentioned above solution containing the UMONs-SH. The solution was vortexed and heated to 70 °C for 45–60 minutes. After cooling down to room temperature, an aliquot was taken for determination of radiochemical purity by radio-TLC using 0.1 mol/L citric acid (pH 5) as a development solvent. The retention factor of  $^{64}\text{Cu}$ -labeled UMONs was  $\sim 0 - 0.1$  and that of free  $^{64}\text{Cu}$  was  $\sim 0.9$ .

**Part B: Supplementary Figures**

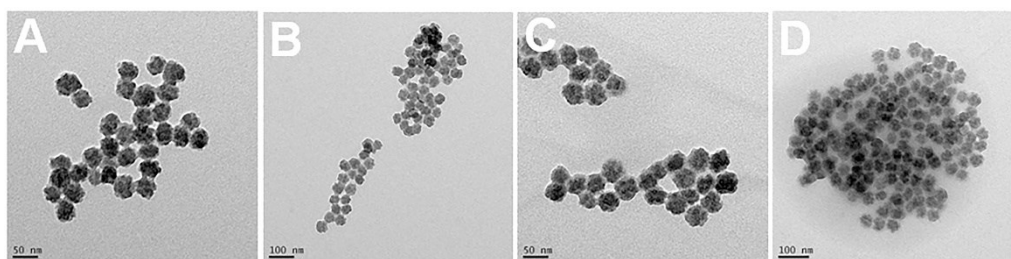


**Figure S1** Observation of the biodegradation behavior of UMons in the absence of GSH solutions. TEM images of UMons in the absence of GSH solutions on (A) Day 1, (B) Day 3, (C) Day 7 and (D) Day 10.

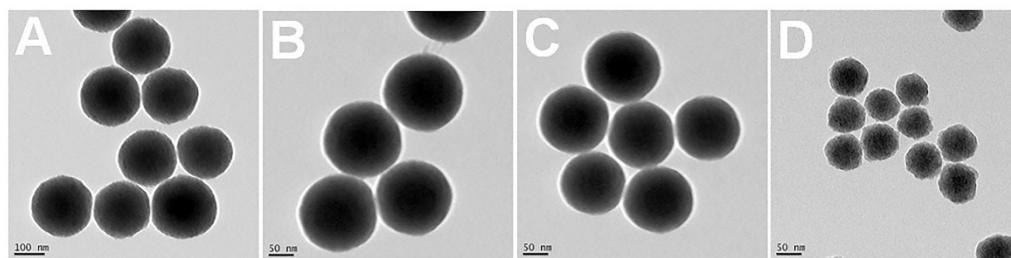


**Figure S2** The diameter of solid organosilica nanoparticles (SONs) was around (A) 200 nm, (B) 165 nm, (C) 150 nm, (D) 50 nm. The different sizes of SONs prepared in a mixture of  $\text{NH}_3 \cdot \text{H}_2\text{O}$ , water and ethanol by adjusting the concentration of  $\text{NH}_3 \cdot \text{H}_2\text{O}$ . The concentrations of  $\text{NH}_3 \cdot \text{H}_2\text{O}$  was from low to high for A-D.

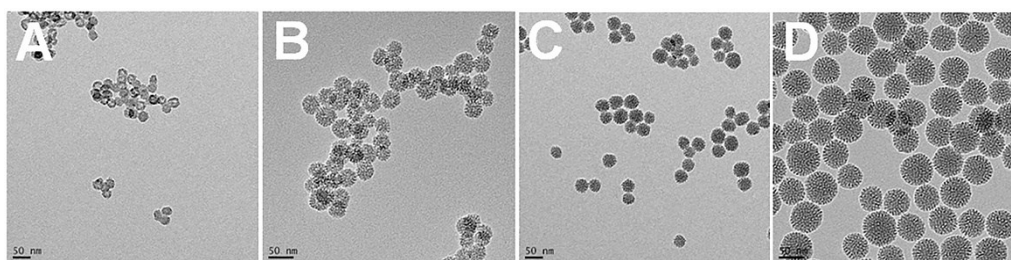


**Figure S3** The diameter of mesoporous organosilica nanoparticles (MONs) was around (A) 25 nm, (B) 34 nm, (C) 40 nm, (D) 50 nm. The MONs were prepared by using CTAC as the pore-making agent and TEA as a catalyst. The concentration of TEA was from high to low for A-D.

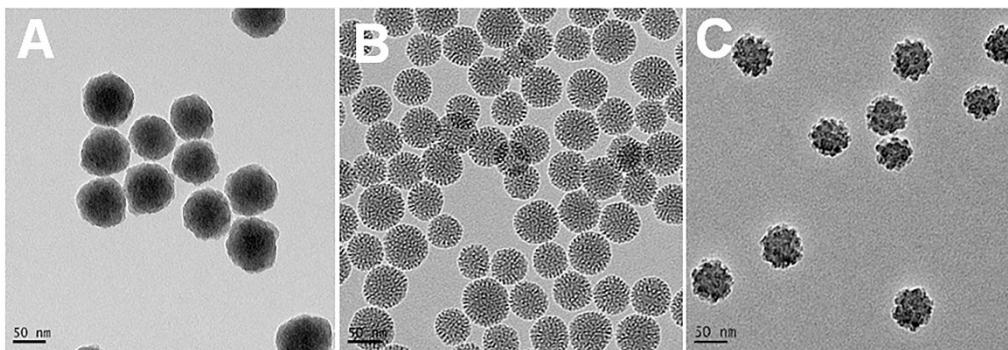


**Figure S4** TEM images of (A) the SONs, (B) MONs, and (C) the UMONs at the same size (50 nm).

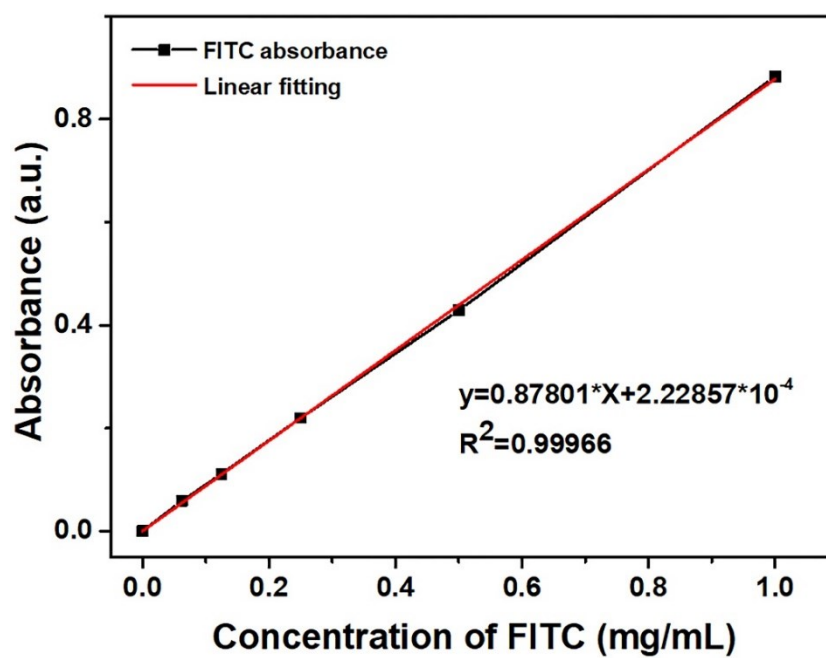


**Figure S5** Standard curve of FITC as a function of mass concentration *via* UV-Vis method.

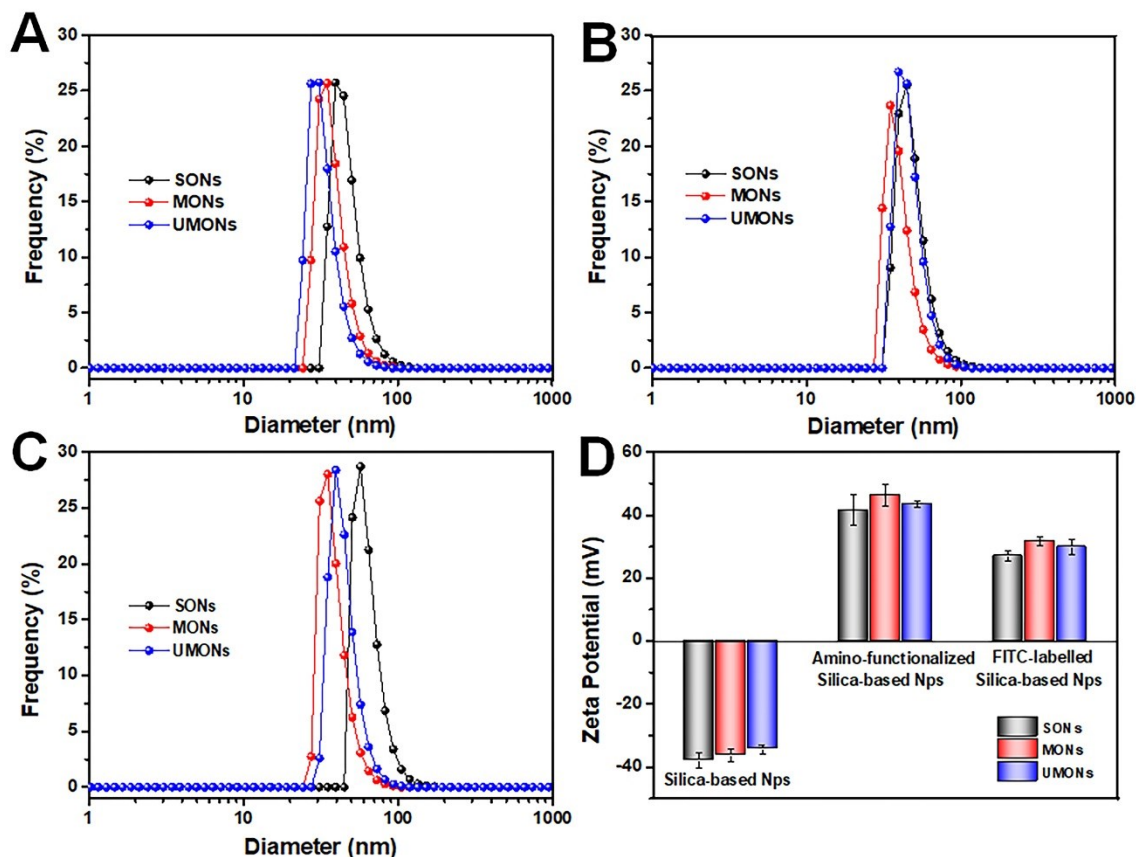


**Figure S6** Size distributions for three types of organosilica nanoparticles in (A) water, (B) PBS and (C) cell media. Due to their similar size and good monodispersity, according to the experimental results, the effects of size-induced and aggregation-state-induced biological behavior can be both ignored in our test system. (D) Zeta potential analysis for the organosilica nanoparticles, amino-functionalized organosilica nanoparticles and FITC-labeled organosilica nanoparticles. It can be seen that there is no significant charge difference between these three samples, suggesting that the effect of zeta-potential-induced bio-behavior can be ignored in our test system.

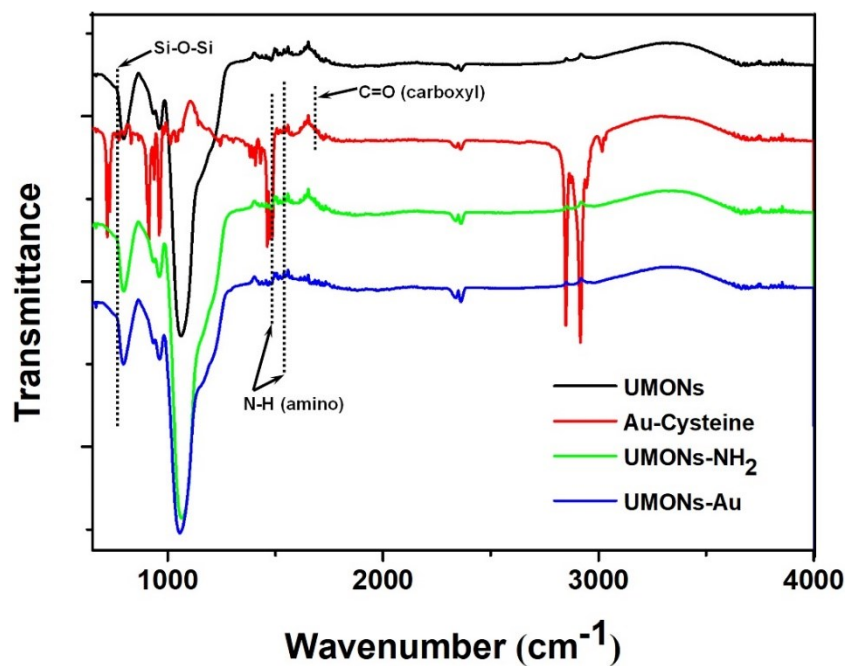


**Figure S7** FT-IR spectra of UMONs, Au-Cysteine, UMONs-NH<sub>2</sub>, and UMONs-Au.

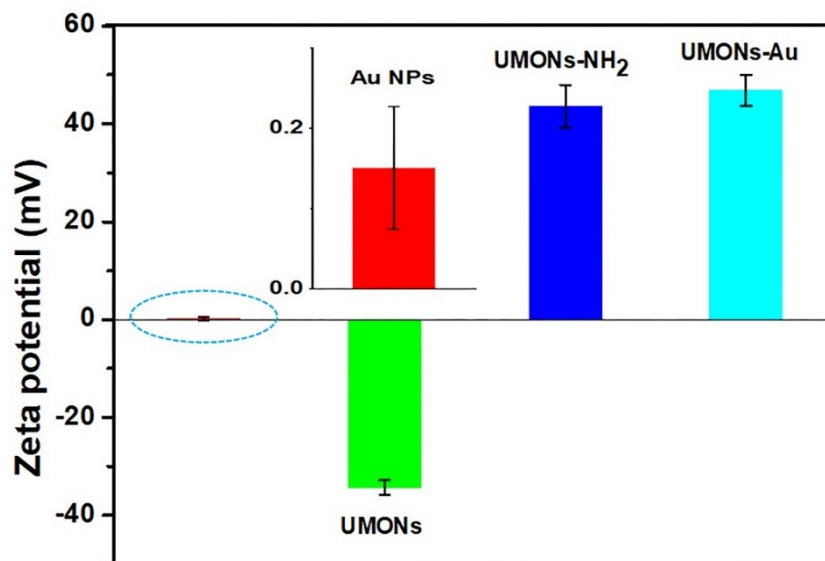


**Figure S8** Zeta potentials of ultrasmall Au NPs, UMONs, UMONs-NH<sub>2</sub>, UMONs-Au.

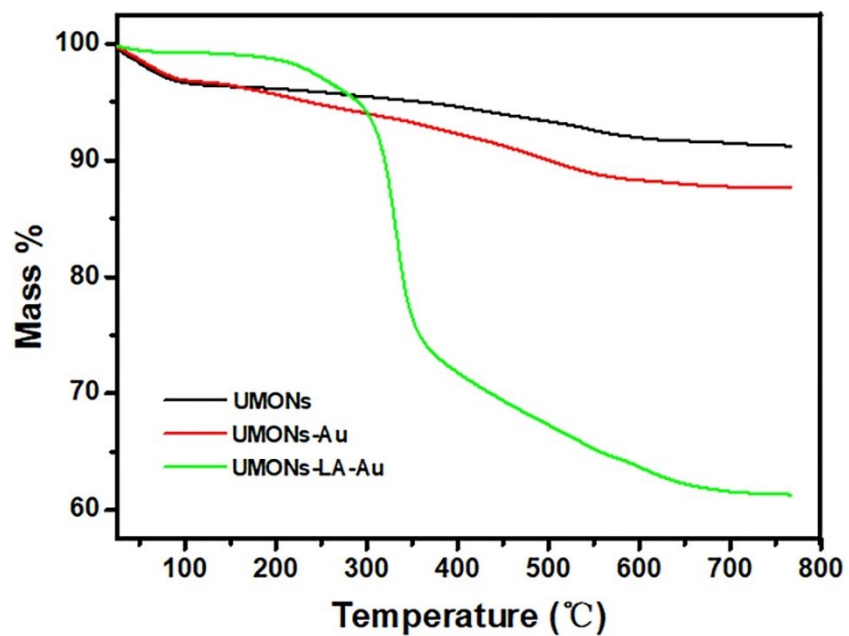


**Figure S9** TGA curves of UMONs, UMONs-Au, and UMONs-LA-Au.

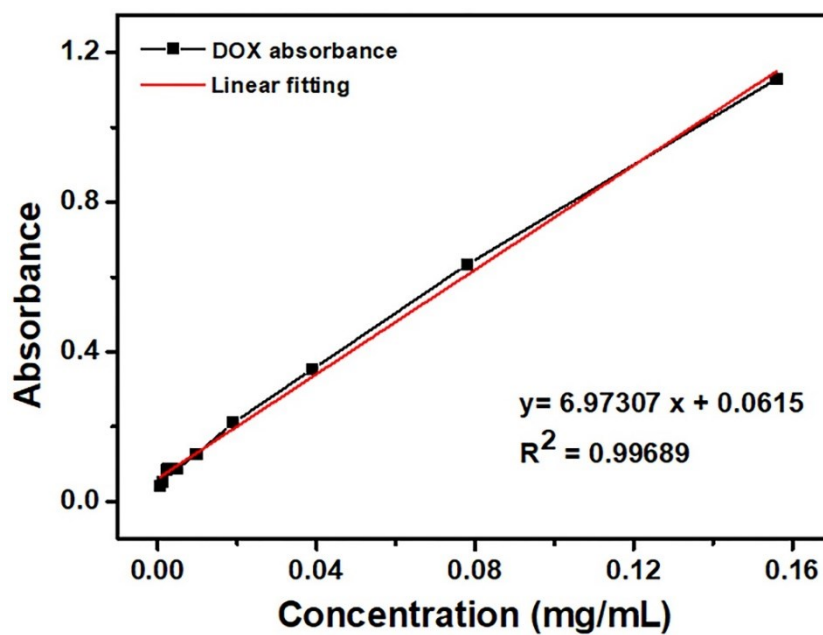


**Figure S10** Standard curve of DOX as a function of mass concentration *via* the UV-Vis method.



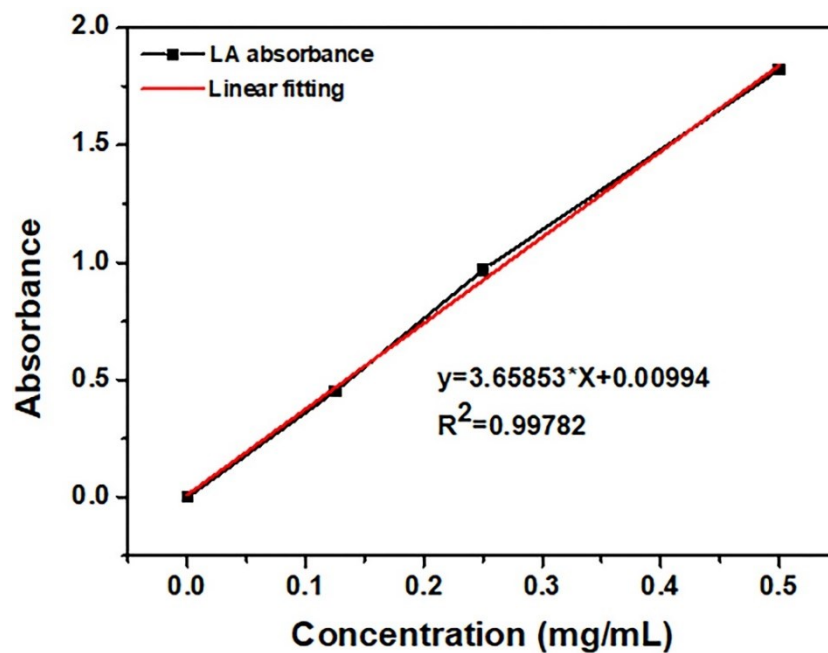


**Figure S11** Standard curve of LA as a function of mass concentration *via* the UV-Vis method.

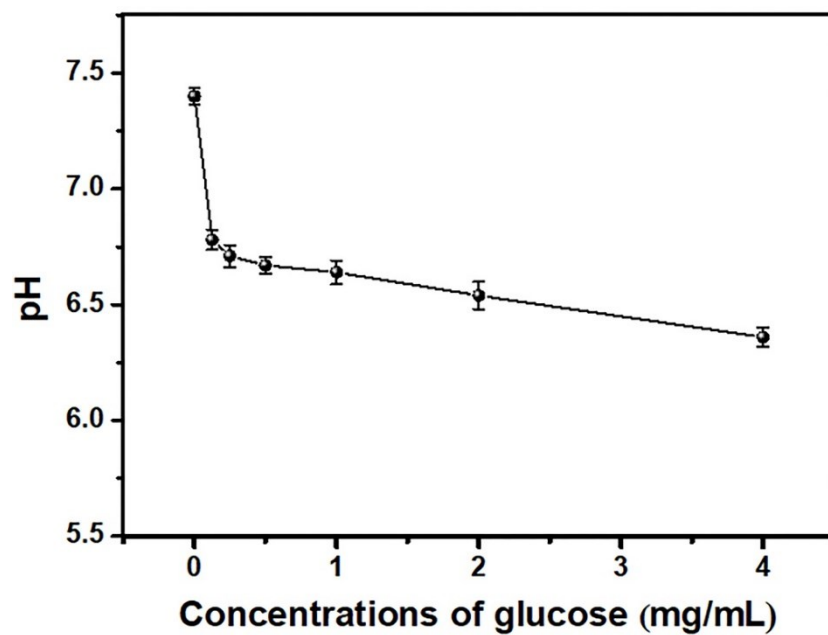


**Figure S12** Variation of pH value at different concentrations of glucose arising from the ultrasmall gold-catalyzed decomposition reaction of glucose.

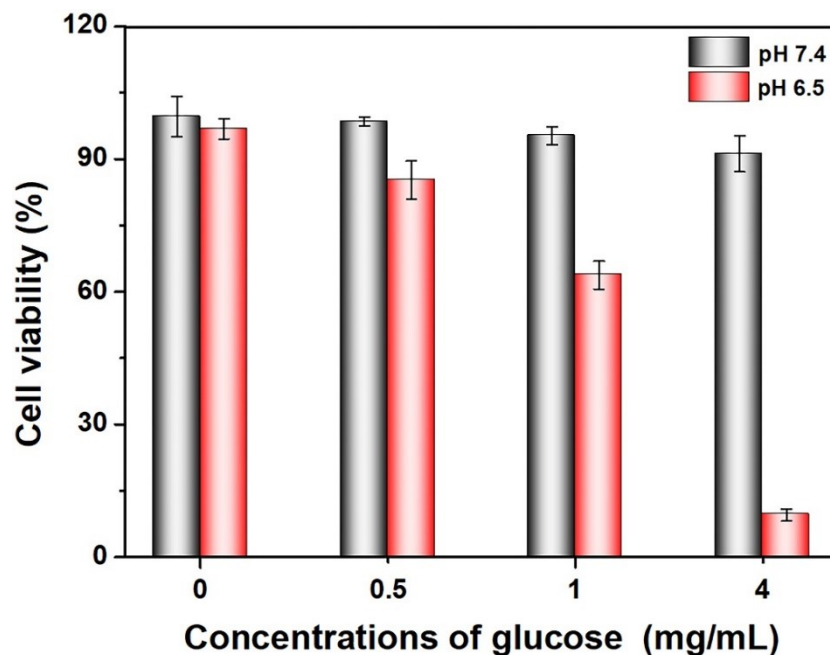


**Figure S13** Viabilities of U87MG cells after incubation with UMONs-LA-Au (200  $\mu\text{g/mL}$ ) in different concentrations of glucose at pH 7.4 and pH 6.5 media, respectively.

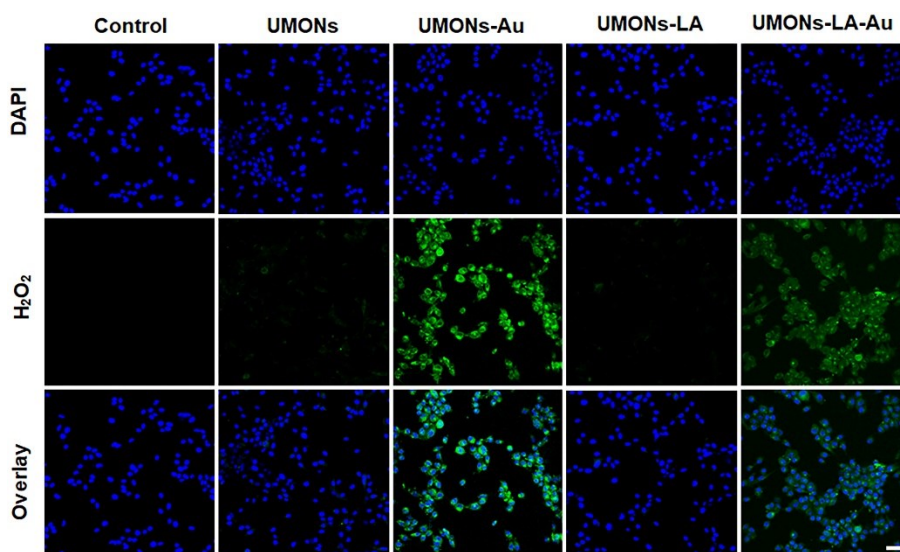


**Figure S14** H<sub>2</sub>O<sub>2</sub> generation after the treatment. Significant amounts of H<sub>2</sub>O<sub>2</sub> were observed in the group treated with UMONs-Au and UMONs-LA-Au, and the UMONs-Au treated group produced more H<sub>2</sub>O<sub>2</sub> than that of UMONs-LA-Au, which may be due to the further LA-H<sub>2</sub>O<sub>2</sub> reaction. Marginal H<sub>2</sub>O<sub>2</sub> signals were observed in the other three control groups. Scale bar, 60  $\mu\text{m}$ .

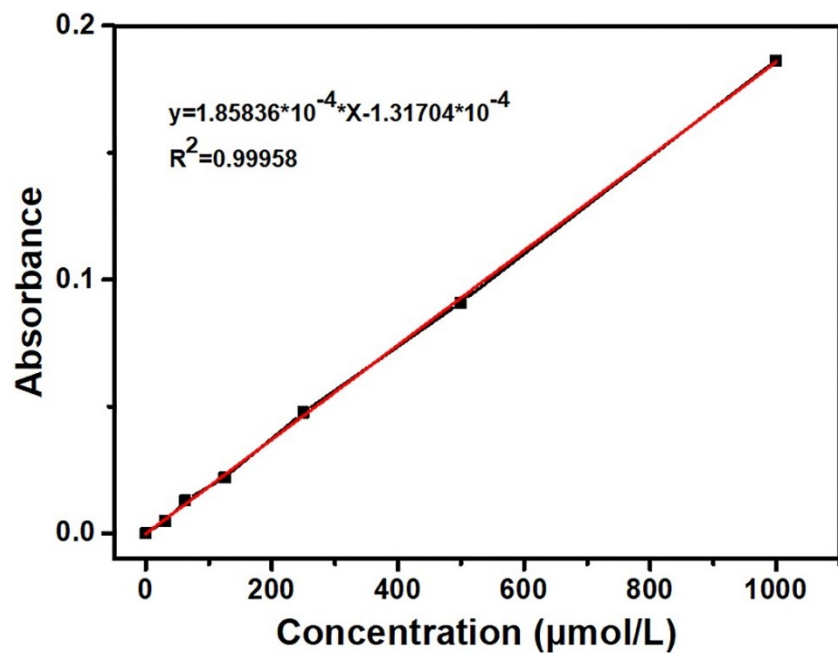


**Figure S15** Standard curve of H<sub>2</sub>O<sub>2</sub> via UV-Vis method.

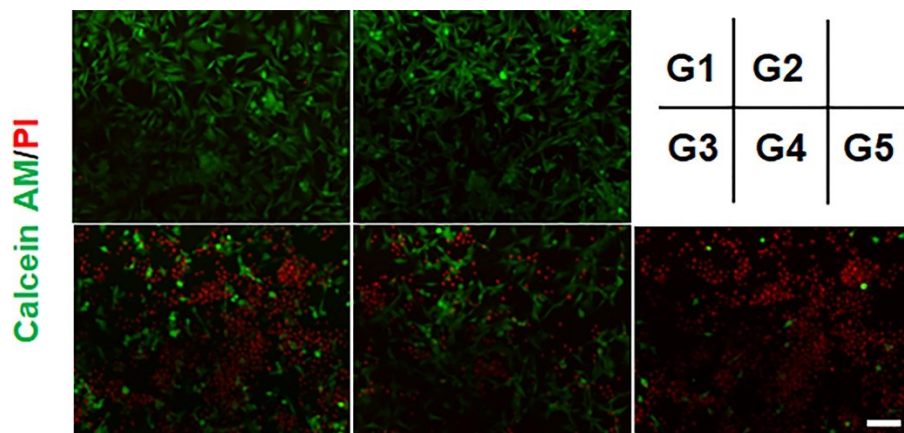


**Figure S16** Live and dead assays. Green, Calcein AM, live cells. Red, PI, dead cells. Scale bar, 100 μm. Cells were co-incubated with the UMONs-LA-Au (G5) as the nanocatalysis-enhanced NO gas therapy. Cells were treated with UMONs-LA and UMONs-Au as the NO gas therapy alone group (G4) and the nanocatalysis alone group (G3), respectively. For other controls, cells were treated with UMONs (G2) only and PBS (G1) only.

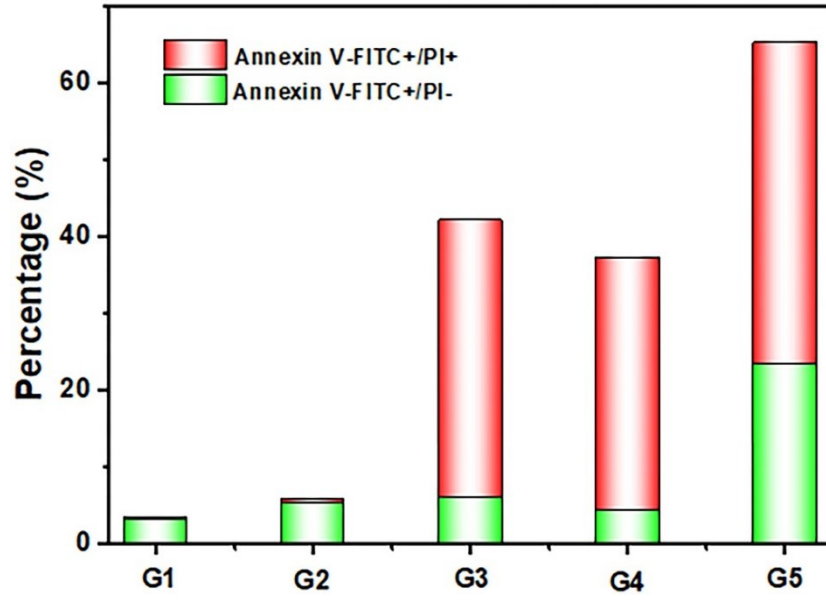


**Figure S17** Quantitative analysis of the corresponding cell apoptosis/necrosis percentages based on flow cytometry analysis of apoptotic/necrotic cells *via* Annexin V-FITC/PI assays.

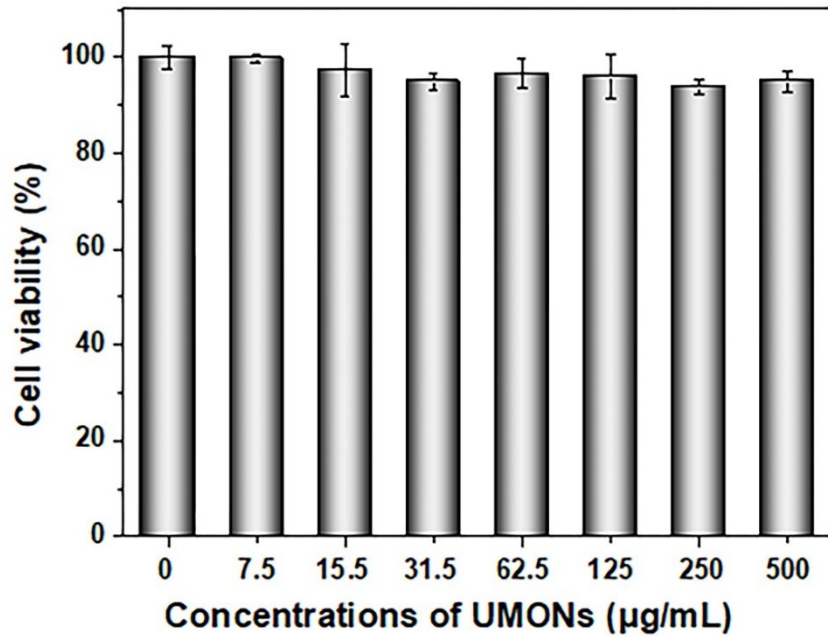


**Figure S18** Viabilities of U87MG cells after 24 h of incubation with different concentrations of UMONs.

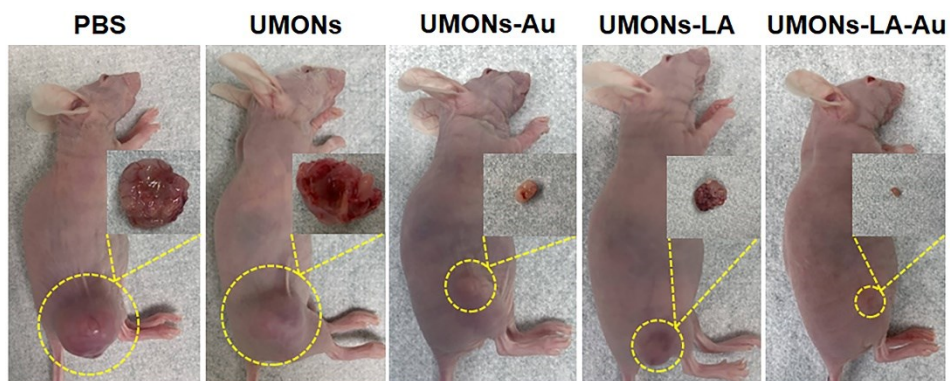


**Figure S19** Representative digital photos of U87MG tumor-bearing nude mice and dissected tumors (insets of S19) on Day 15.

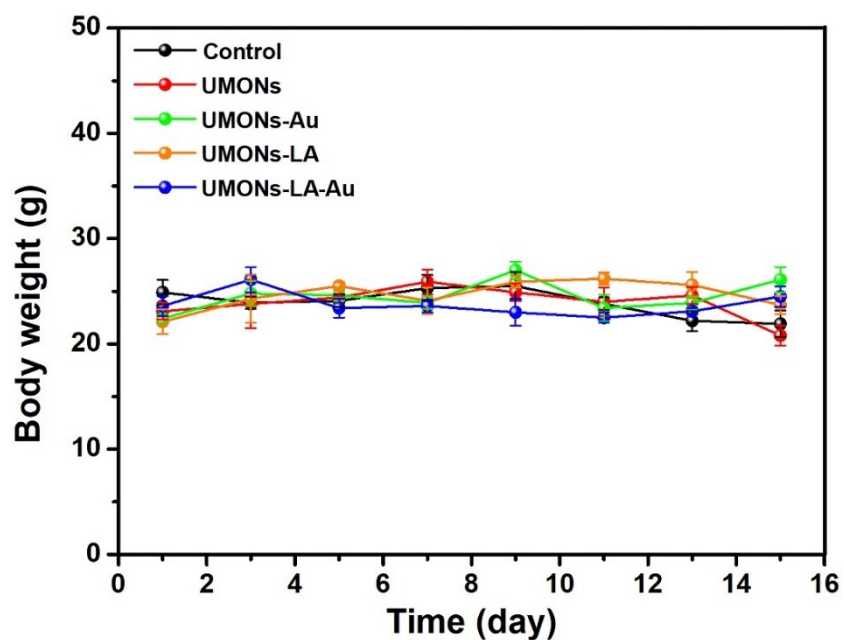


**Figure S20** Time-dependent body-weight curves of U87 MG tumor-bearing nude mice subjected to different treatments.

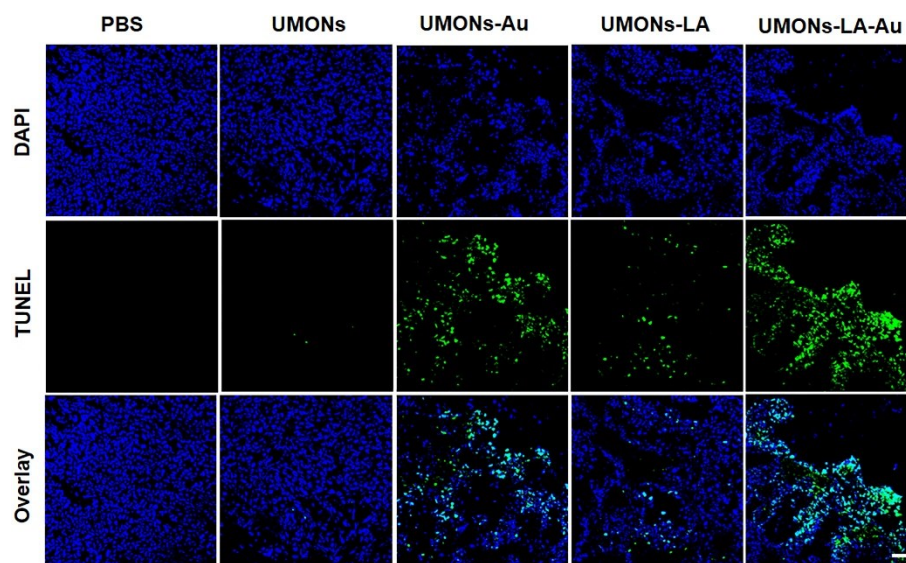


**Figure S21** Images of TUNEL stained sections of tumors from the different groups on Day 15 after administration. Scale bar: 100  $\mu$ m.

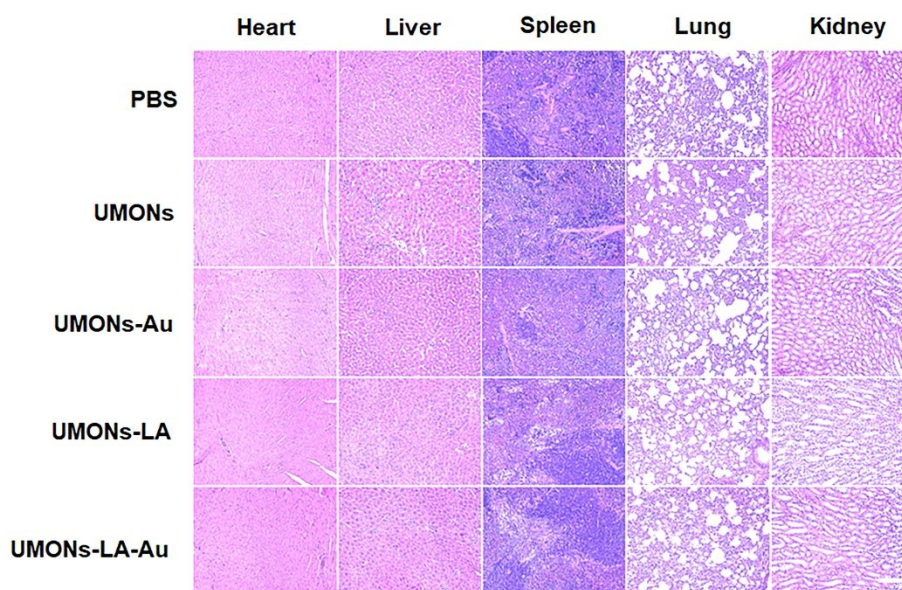


**Figure 22** Hematoxylin & eosin (H & E)-stained tissue images of the major organs (heart, liver, spleen, lung, and kidney) extracted from the female nude mice after various treatments, indicating that these treatments have relatively low side effects on the mice health. Scale bar, 100  $\mu$ m.